

# On Certain Noise Filtering Techniques in Fixed Point Iteration-based Adaptive Control\*

Hazem Issa<sup>a</sup>

<sup>a</sup>Doctoral School of Applied Informatics and Applied Mathematics  
Óbuda University  
Budapest, Hungary  
hazem.issa@uni-obuda.hu

Mahmod Al-Bkree

Bánki Donát Faculty of Mechanical and Safety Engineering  
Óbuda University  
Budapest, Hungary  
albkriengineer@gmail.com

József K. Tar<sup>a,b,c</sup>

<sup>b</sup>John von Neumann Fac. of Informatics  
<sup>c</sup>ABC iRob  
Óbuda University  
Budapest, Hungary  
tar.jozsef@nik.uni-obuda.hu

**Abstract**—In control applications the use of noise-burdened sensor signals cannot be evaded. Also, certain signals can be lost. This problem traditionally is tackled by the use of Kalman filters that provide some “optimal solution” to these problems based on reasonable assumptions that are not always well underpinned in the practice. These are assumptions are made with regard to the system model and the statistical distribution of the noise signals. The Fixed Point Iteration-based adaptive controller is applicable for various strongly nonlinear models. Because feeding back the order of time-derivative of the system’s variable that immediately can be varied by the control signal, its noise sensitivity can be considerable. In this paper the operation of an unscented Kalman filter-based technique is compared with that of a simple moving window with affine signal approximation, and the use of a third order low pass filter in the control of a modified van der Pol oscillator. In this model a quadratic drag term is added to the original model to describe the motion of the system in turbulent fluid environment. According to the numerical simulations it can be stated that the simpler methods can replace the more complicated Kalman filter.

**Index Terms**—unscented kalman filter, fixed point iteration-based adaptive control, nonlinear dynamic systems, noise filtering

## I. INTRODUCTION

The usual “Resolved Acceleration Rate Controllers” (e.g., [1]–[3]) normally apply the feedback of the tracking error, its time-integral, and first time-derivative. The measurement noise if their input may be considerable. The “Acceleration Feedback Controllers” that are in use from the Nineties of the past century (e.g., [4]–[7]). Since they also feed back a second order derivative, they may be even more noise sensitive solutions. The “Fixed Point Iteration-based Adaptive Controllers (FPIADC)” introduced in 2009 in [8], and sketched in Fig. 1 also feed back the second time-derivative of the controlled variably. Consequently, the noisy nature of this signal may cause practical problems and may require efficient noise filtering solutions in the case of this controller, too.

The present paper is an extended version of the conference publication [9] in which preliminary steps were made for the investigations aiming at the applicability of Kalman filter for our purposes.

We acknowledge the support of this work by the Doctoral School of Applied Informatics and Applied Mathematics of Óbuda University.

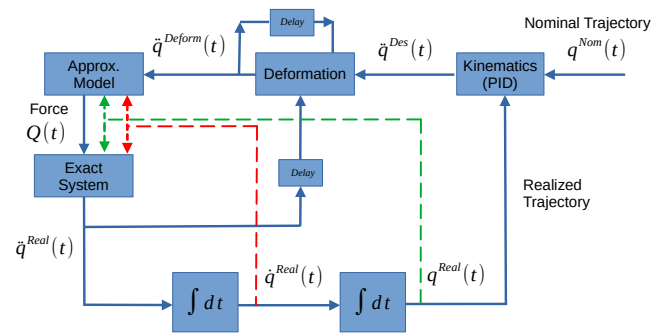


Fig. 1. The schematic structure of the “Fixed Point Iteration-based Adaptive Controller” for a second order dynamical system (after [8])

According to Fig. 1, it is assumed that variable  $q(t)$  can be measured with an additive noise term  $\mathcal{N}(t)$  therefore the observed coordinate is modeled as  $q^o(t) = q(t) + \mathcal{N}(t)$ . In the block “Kinematics (PID)” for instance a PID-type error feedback can be formulated according to (1) that is able to asymptotically drive the tracking error to zero if it is precisely realized

$$e(t) := q^N(t) - q(t), \quad e_{int}(t) := \int_{t_0}^t e(\xi) d\xi, \quad (1)$$

$$\left(\Lambda + \frac{d}{dt}\right)^3 e_{int}(t) \equiv 0 \text{ yielding}$$

$$\ddot{q}^{Des}(t) = \ddot{q}^N(t) + \Lambda^3 e_{int}(t) + 3\Lambda^2 e(t) + 3\Lambda \dot{e}(t).$$

In (1) the integral, the order zero, and the first time-derivatives of the noisy signal  $q(t)$  occur in the feedback loop of the PID-type controller. In the block “Deformation” an appropriate function

$$\ddot{q}^{Def}(t + \tau) = G(\ddot{q}^{Def}(t), \dot{q}(t), \ddot{q}^{Des}(t + \tau)) \quad (2)$$

can be applied by the use of which on the basis of the observed behavior of the controlled system at time instant  $t$  (i.e., the realized  $\ddot{q}(t)$  system response that was obtained for the deformed control signal  $\ddot{q}^{Def}(t)$ ), and the kinematically designed desired value for  $t + \tau$  are utilized in the calculation of the next deformed value  $\ddot{q}^{Def}(t + \tau)$ . Since normally both

the *Exact Model's* and the available *Approximate Model's* response depend on the actual  $q(t)$  and  $\dot{q}(t)$  values, it can be written that

$$\ddot{q}(t) = f(\ddot{q}^{Def}(t), q(t), \dot{q}(t)) \cong f(\ddot{q}^{Def}(t)) \quad , \quad (3)$$

since  $\ddot{q}^{Def}(t)$  can be abruptly modified by the controller while  $q(t)$  and  $\dot{q}(t)$  can vary only slowly, consequently they can be considered rather as “*parameters*” than “*variables*” of this function. In this approximation (2) can be written as

$$\ddot{q}^{Def}(t + \tau) = G(\ddot{q}^{Def}(t), f(\ddot{q}^{Def}(t)), \ddot{q}^{Des}(t + \tau)) \quad , \quad (4)$$

the parameters of which are slowly varying. In the case of a digital controller, the minimal possible delay time  $\tau$  is the duration of one digital control cycle. The transformation of the task of finding the appropriate  $\ddot{q}_*$  deformed input signal in (4) into a fixed point problem so that

$$\ddot{q}_* = G(\ddot{q}_*, f(\ddot{q}_*), \ddot{q}^{Des}) \quad \text{while} \quad f(\ddot{q}_*(t)) = \ddot{q}^{Des}(t) \quad (5)$$

was called as *fixed point transformation*. For this purpose various possible solutions were suggested (e.g., in [8], [10]–[13]). The parameters of the function in (4) must be so chosen that around the fixed point of the function, i.e.,  $\ddot{q}_*$   $G$  must be contractive for the given  $\ddot{q}^{Des}(t)$ . Then, according to Banach's fixed point theorem [14] the sequence  $\{\ddot{q}_{i+1}^{Def} = G(\ddot{q}_i^{Def}, f(\ddot{q}_i^{Def}), \ddot{q}^{Des}(t))\}$  with the initial element  $\ddot{q}_1^{Def} = \ddot{q}^{Des}(t)$  converges to the unique solution:  $\ddot{q}_i^{Def} \rightarrow \ddot{q}_*$ . For guaranteeing contractivity the free parameters of function  $G$  must be appropriately set. Because during one digital control step only one step of this adaptive iteration can be done, in the practice it converges during a few steps that does not mean problem because according to the kinematic design  $\ddot{q}^{Des}(t)$  varies only slowly. Following the initial phase of convergence  $\ddot{q}^{Des}(t)$  “*drags*” with itself  $\ddot{q}_*(t)$ . For obtaining precise trajectory tracking beside the *fact of convergence* its *speed* is an important factor: the “*dynamics*” of  $\ddot{q}^{Des}(t)$  must be tracked with appropriate speed.

The noise-sensitivity of this method originates from two essential sources:

- from the kinematic design in (1): the controller may have precise information on the nominal trajectory, therefore  $\ddot{q}^N(t)$ ,  $\dot{q}^N(t)$ , and  $q^N(t)$  are precisely known but the actual values  $q(t)$ ,  $\dot{q}(t)$ , and  $\ddot{q}(t)$  are not known; instead of  $q(t)$  its noisy measured value  $q^o(t)$  is available, and in the place of  $\dot{q}^o(t)$  some estimated values must be put;
- also, in the adaptive feedback, in the place of  $\ddot{q}(t)$  some estimation of  $\ddot{q}^o(t)$  must be put.

In the sequel at first two “*simple*” filtering techniques will be considered, and finally an attempt is made for the use of an unscented Kalman filter.

## II. THE NOISE FILTERING TECHNIQUES INVESTIGATED

As in the preliminary conference version of the present paper, i.e., in [9] the variants as follows were investigated.

### A. Application of Moving Window with Affine Signal Approximation

For averaging out the consequences of noisy measurement, in [13] a moving window of buffer length  $L \in \mathbb{N}$  was introduced. It was filled in with the latest observed values as  $\{q^o(t_{i-L+0}), q^o(t_{i-L+1}), \dots, q^o(t_{i-L+L})\}$ , i.e.,  $\{q^o(t_{i-L+m})\}$ ,  $m = 0, 1, \dots, L$ . The content of this window was approximated with an *affine model form*  $\{a_0 m + b_0\}$  that allows a “*filtered*” identification of the first time-derivative related to the coefficient  $a_0$ . After fitting the parameters  $a_0$ ,  $b_0$  with the least squares error, the smoothed value  $\tilde{q}^o(i) = a_0 L + b_0$  was chosen at the end of the window. For the filtered approximation  $\tilde{q}^o(t_i) = \frac{q^o(t_i) - \tilde{q}^o(t_{i-1})}{\delta t_i}$  was chosen. Following that, the above calculated  $\tilde{q}^o(t_i)$  values were put into the grid points  $\{\tilde{q}^o(t_{i-L+0}), \tilde{q}^o(t_{i-L+1}), \dots, \tilde{q}^o(t_{i-L+L})\}$ , and were approximated with the same affine form as  $\{a_1 m + b_1\}$ . The term  $\tilde{\tilde{q}}^o(t_i) = a_1 L + b_1$  provided the filtered derivatives as  $\tilde{\tilde{q}}^o(t_i)$ . This scheme was continued for obtaining the filtered substitute of  $\ddot{q}^o(t)$ .

In this case a special fixed point iteration was applied that operated with the time-derivative of the deformed second derivative generalized coordinate as in [13] as

$$\begin{aligned} \frac{d\ddot{q}^{Def}}{dt} &:= \frac{A}{\tau} \sigma \left( \frac{f(\ddot{q}^{Def}(i)) - \ddot{q}^{Des}}{w} \right) \approx \\ &\approx \frac{\ddot{q}^{Def}(i+1) - \ddot{q}^{Def}(i)}{\tau} \quad , \end{aligned} \quad (6)$$

in which  $\sigma(x) = \frac{x}{1+|x|}$  is a *sigmoid function*, parameter  $w$  determines its steepness, and for  $\mathbb{R} \ni A < 0$  can cause an approximately exponential decrease of the argument. In the simulations  $\tau = \delta t = 10^{-3}$  s,  $w = 3\text{m} \cdot \text{s}^{-2}$ ,  $A = -1.1\text{s}^{-2}$ , and  $\Lambda_{FPI-1} = 24.0\text{s}^{-1}$  in (1). The length of the digital filter was  $L = 12$  steps.

### B. Application of an Efficient Third Order Low Pass Filter

In this case the noisy signal  $q^o(t) = q(t) + \mathcal{N}(t)$  was tracked according to the differential equation

$$\left( \lambda_{FPI-2} + \frac{d}{dt} \right)^3 \ddot{q}^o(t) = \lambda_{FPI-2}^3 q^o(t) \quad , \quad (7)$$

with the initial conditions  $\ddot{q}^o(t_0) = 0$ ,  $\dot{q}^o(t_0) = 0$ , and  $q^o(t_0) = 0$ . This idea was borrowed from [15]. Evidently, at zero frequency it has the transfer function value 1, while for high frequencies it is  $\propto s^{-3}$  for the variable of the Laplace transform, i.e., it realizes drastic suppression for the high frequency components. In the block “*Kinematics (PID)*” of Fig. 1 the appropriate exponent in (1) was  $\Lambda_{FPI-2} = 16.0\text{s}^{-1}$ ,  $\lambda_{FPI-2} = 350.0\text{s}^{-1}$  was in use. The “*Fixed Point Transformation Function*” applied in the block “*Deformation*” of Fig. 1 in this case was the original “*Robust Fixed Point Transformation*” published in [8] as

$$\begin{aligned} \ddot{q}^{Deform}(t_{i+1}) &= (\ddot{q}^{Deform}(t_i) + K_c) \cdot \\ &[1 + B_c \sigma(A_c [f(\ddot{q}^{Deform}(t_i)) - \ddot{q}^{Des}(t_{i+1})])] - K_c \end{aligned} \quad (8)$$

in which the same sigmoid function was in use as in (6), and in the simulations  $K_c = 4 \times 10^7 \text{ m} \cdot \text{s}^{-2}$ ,  $B_c = -1.05$ , and  $A_c = \frac{9 \times 10^{-2}}{K_c} \text{ m}^{-1} \cdot \text{s}^2$  were applied.

### C. Unscented Kalman Filter

The Unscented Kalman Filter is widely used for estimation in the case of nonlinear systems wherever the full state feedback is required. Its essence is the nonlinear “*Unscented Transformation*” that calculates the statistical properties for an arbitrary random variable [16]–[19]. In this approach the nonlinear system is described as function of firstly the input state variables  $q_k$  in addition with which the process noise  $w_{k-1}$  is considered, and secondly, the observed values or the system measurements  $y_k$  to which also is added a so called “*sensor noise*” or “*measurement noise*”  $v_k$  in (9) as

$$q_k = f(q_{k-1}, u_{k-1}) + w_{k-1} , \quad (9a)$$

$$z_k = h(q_k) + v_k . \quad (9b)$$

In this paper a strictly causal process was assumed with  $w_k = 0$ , furthermore, it was assumed that the variables were directly measurable, i.e.,  $z_k \equiv h(q_k) = q_k + v_k$  was assumed. For the discretized dynamic model (i.e., for the first equation of (9)) the approximation

$$\dot{q}_j \approx \dot{q}_{j-1} + \frac{\delta t}{m} (-kq_j - b(q_j^2 - a^2)\dot{q}_j + u_j) , \quad (10)$$

$$q_j \approx q_{j-1} + \delta t \dot{q}_j ,$$

was applied on the basis of the dynamic model of the controlled system in (11) that is the extension of the original van der Pol oscillator [20] by adding the term  $dsign(\dot{q})\dot{q}^2$  to its equation of motion as

$$m\ddot{q} + kq - b_1(a^2 - q^2)\dot{q} + b_2\dot{q} + dsign(\dot{q})\dot{q}^2 = u \quad (11)$$

with the model parameters given in Table I. (The original system physically was an externally excited triode. For the sake of simplicity here it is considered as a “mechanical” one.)

TABLE I  
THE SYSTEM PARAMETERS

Parameter	Exact Value	Approx Value
Mass $m$ [kg]	1.5	2.0
Spring stiffness $k$ [N · m <sup>-1</sup> ]	125.0	150.0
Separator $a$ [m]	2.1	1.2
Damp./Excit. coeff. $b_1$ [N · s · m <sup>-3</sup> ]	0.6	1.5
Damping coeff. $b_2$ [N · s · m <sup>-1</sup> ]	3.5	2.5
Quadr. damp. coeff. $d$ [N · s <sup>2</sup> · m <sup>-3</sup> ]	4.3	1.3

The “*Extended Kalman Filter (EKF)*”, in general, applies the first order Taylor series approximation of the functions in (9), therefore it is rather appropriate to tackle slight nonlinearities. The new idea announced in [21] was that instead using the Jacobians of the functions in (9), the state distribution was specified by a minimal set of deterministically chosen sample points of a Gaussian random variable (the so called “*sigma points*”), and these points were propagated through the

nonlinear system. In this manner a better approximation was obtained for the posterior mean and covariance that resulted by the use of the Jacobians.

In our case the state vector is physically defined as  $q(k) = [\dot{q}_k, q_k]$ , and the initial conditions of the mean is  $\hat{q}_0 = E[q_0]$  with the initial covariance  $P_0 = E[(q_0 - \hat{q}_0)(q_0 - \hat{q}_0)^T]$ . In every cycle the sigma points of the probability density distribution (it is tacitly assumed to be Gaussian or “Normal” distribution) are calculated for  $L = 2$  as

$$\begin{aligned} \chi_{k-1} = & [\hat{q}_{k-1} , \\ & \hat{q}_{k-1} + \sqrt{(1+\lambda)P_{k-1}}, \hat{q}_{k-1} + \sqrt{(2+\lambda)P_{k-1}}, \\ & \hat{q}_{k-1} - \sqrt{(1+\lambda)P_{k-1}}, \hat{q}_{k-1} - \sqrt{(2+\lambda)P_{k-1}}] \end{aligned} \quad (12)$$

where  $\hat{q}_{k-1}$  is a matrix of size  $2 \times 1$ , and the sigma points are calculated by adding and subtracting to it the appropriate columns of the “*Lower Triangle Cholesky Factorization Matrix*” [22]. The definition of the parameters are given in Table II. The dynamic model  $f(q_k, u_k)$  is evaluated via the sigma points as  $\chi_{k|k-1}^* = f(\chi_{k-1}, u_{k-1})$ . The values of the estimated prior state and covariance are computed by multiplying their values by the weighted sample means  $W_i^m$  and  $W_i^c$  in (13)

$$\begin{aligned} \hat{q}_k^- &= \sum_{i=0}^{2L} W_i^m \chi_{i,k|k-1}^* \\ P_{k|k-1}^- &= \sum_{i=0}^{2L} W_i^c [\chi_{i,k|k-1}^* - \hat{q}_k^-][\chi_{i,k|k-1}^* - \hat{q}_k^-]^T + \\ &+ Q_{Noise} . \end{aligned} \quad (13)$$

The process noise covariance  $Q_{Noise} \in \mathbb{R}^{2 \times 2}$  where it is set to be  $[10^{-1}; 10^{-3}]$ .

TABLE II  
THE UKF SCALING PARAMETERS

Parameter	Description	Value
$\alpha$	Primary Scaling	$10^{-2}$
$\beta$	Secondary Scaling	$10^{-3}$
$\kappa$	Scalar	0.0
$L$	State vector Dimension	2
$\lambda$	Scalar	$\alpha^2(L + \kappa) - L$
$W_0^m$	Initial State Weight	$\frac{\lambda}{L + \lambda}$
$W_i^m$	State Weight	$\frac{1}{2(L + \lambda)}$
$W_0^c$	Initial Covariance Weight	$\frac{\lambda}{L + \lambda} + (1 - \alpha + \beta)$
$W_i^c$	Covariance Weight	$\frac{1}{2(L + \lambda)}$
$\Lambda_{UKF}$	Positive constant in(1) [s <sup>-1</sup> ]	36.0

Following that, UKF starts the correction phase for  $L = 2$  as

$$\begin{aligned} \chi_{k|k-1} := & [\hat{q}_{k-1}^-, \hat{q}_{k-1}^- + \\ & + \sqrt{(1+\lambda)P_{k-1}^-}, \hat{q}_{k-1}^- + \sqrt{(2+\lambda)P_{k-1}^-} \\ & \hat{q}_{k-1}^- - \sqrt{(1+\lambda)P_{k-1}^-}, \hat{q}_{k-1}^- - \sqrt{(2+\lambda)P_{k-1}^-}] . \end{aligned} \quad (14)$$

Then the unscented transformation is done over the observed values i.e., the sigma points are calculated by the function

of  $\gamma_{k|k-1} = h(\chi_{k|k-1})$  and then recombined to produce the predicted measurement values  $\hat{z}_k^- = \sum_{i=0}^{2L} W_i^m \gamma_{i,k|k-1}$  and the predicted measurement covariance

$$P_{z_k^- z_k^-} = \sum_{i=0}^{2L} W_i^c [\gamma_{i,k|k-1} - \hat{z}_k^-][\gamma_{i,k|k-1} - \hat{z}_k^-]^T + R_{Noise} \quad (15)$$

where the measurement noise covariance  $R_{Noise} \in \mathbb{R}^{2 \times 2}$  were set to  $[10^{-2}; 10^{-3}]$ . The “trading values” between the state and measurement are obtained by calculating the cross covariance in (16)

$$P_{q_k z_k} = \sum_{i=0}^{2L} W_i^c [\chi_{i,k|k-1} - \hat{q}_k^-][\gamma_{i,k|k-1} - \hat{z}_k^-]^T \quad (16)$$

that allows the computation of the Kalman gain  $K_{gain} = P_{q_k z_k} P_{z_k z_k}^{-1}$  yielding the updated state variables and covariance values as

$$\hat{q}_k = \hat{q}_k^- + K_{gain} (\hat{z}_k - \hat{z}_k^-) \quad (17a)$$

$$P_k = P_k^- - K_{gain} P_{z_k^- z_k^-} K_{gain}^T \quad (17b)$$

Normally it is not easy to find appropriate values for  $Q_{Noise}$ , and  $R_{Noise}$ . The literature generally recommends the use of small (not zero) values the effects of which spread toward (13) and (15). For making the most possible correct comparison their values must be experimentally set achieve the best behavior of the Kalman filter.

Because our system is a second order one, the noise distributions for  $q(t)$  and  $\dot{q}(t)$  cannot be considered quite independent. For instance, the latter term can inherit certain features if  $\dot{q}(t)$  is numerically computed from  $q(t)$ . This issue is considered in the sequel.

1) *Assumptions Regarding the Inherited Noise Distributions in UKF:* In our paper, for the first derivative of the coordinate value the following assumptions were utilized:

- Let  $x_i$  denote the actual coordinate value at time instant  $t_i$  and let  $\hat{x}_i := x_i + \mu_i$  be its noisy measured value that later will be used for numerical differentiation. It is assumed that  $\forall t_i$  the probability density distribution of the additive noise component is  $\varphi(\mu)$ .
- Then by definition

$$E(\mu) := \int \mu \varphi(\mu) d\mu, \quad (18a)$$

$$\sigma^2(\mu) := \int \varphi(\mu) (\mu - E(\mu))^2 d\mu, \quad (18b)$$

$$\int \varphi(\mu) d\mu = 1. \quad (18c)$$

where the assumption  $E(\mu) = 0$  is reasonable, and it leads to  $\sigma^2(\mu) = \int \varphi(\mu) \mu^2 d\mu$ .

- Let  $\psi(\mu_i, \mu_{i-1})$  denote the probability density distribution of the measurements made in time instants  $t_i$  and  $t_{i-1}$ . If  $\delta t$  is the time-resolution of the discrete differ-

entiation then the mean of the time-derivative computed from the measured values will be

$$\begin{aligned} E\left(\frac{q_i - q_{i-1}}{\delta t}\right) &= \\ &= \int \int \psi(\mu_i, \mu_{i-1}) \frac{x_i + \mu_i - x_{i-1} - \mu_{i-1}}{\delta t} d\mu_i d\mu_{i-1}, \\ &\int \int \psi(\mu_i, \mu_{i-1}) d\mu_i d\mu_{i-1} = 1. \end{aligned} \quad (19)$$

- For independent measurements necessarily  $\psi(\mu_i, \mu_{i-1}) = \varphi(\mu_i) \varphi(\mu_{i-1})$  that yields

$$\begin{aligned} E\left(\frac{x_i - x_{i-1}}{\delta t}\right) &= 1 \frac{x_i - x_{i-1}}{\delta t} + 1E\left(\frac{\mu_i}{\delta t}\right) \\ &- 1E\left(\frac{\mu_{i-1}}{\delta t}\right) = \frac{x_i - x_{i-1}}{\delta t}. \end{aligned} \quad (20)$$

- For the calculation of the standard deviation it is obtained that

$$\begin{aligned} &\int \int \psi(\mu_i, \mu_{i-1}) \left( \frac{x_i + \mu_i - x_{i-1} - \mu_{i-1}}{\delta t} - \frac{(x_i - x_{i-1})}{\delta t} \right)^2 d\mu_i d\mu_{i-1} = \\ &= \int \int \psi(\mu_i, \mu_{i-1}) \left( \frac{\mu_i - \mu_{i-1}}{\delta t} \right)^2 d\mu_i d\mu_{i-1} \\ &= \int \int \varphi(\mu_i) \varphi(\mu_{i-1}) \frac{\mu_i^2 + \mu_{i-1}^2 - 2\mu_i \mu_{i-1}}{\delta t^2} d\mu_i d\mu_{i-1} \\ &= 2 \frac{\sigma^2(\mu)}{\delta t^2} \end{aligned} \quad (21)$$

It must be noted that in the case of the first two methods the “process noise” was not interpreted, only the “observation noise” had physical meaning, i.e., the process was considered strictly causal.

### III. SIMULATIONS

The simulations were made with discrete time resolution  $\delta t = 10^{-3}$  s. In contrast to the original conference paper [9] the nominal trajectory was not a simple sinusoidal function of time. It also contained nonlinear “quasi edges” or “corners” around which drastic variations occurred in its time-derivative. Simulations were made for noise-free case, for “small noise amplitude” and “big amplitude” noise disturbances.

#### A. Default Comparisons: Noise-free Case

To study the “distorting nature” of the noise filtering methods applied figures 2,3,4 were created. They reveal that comparable results were obtained. The fluctuation that is observable at the *FPI-1* is the property of the “continuous fixed point iteration method”.

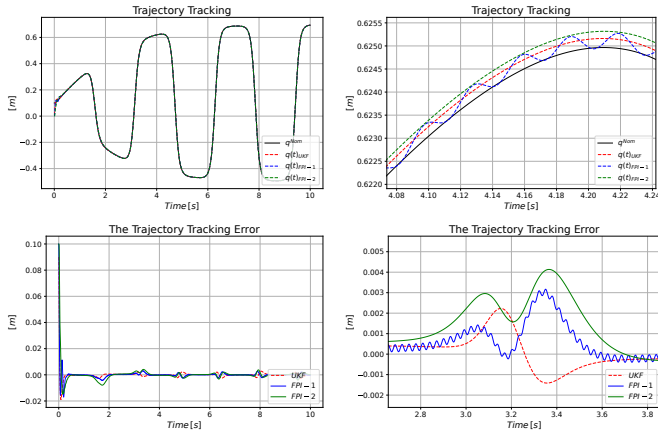


Fig. 2. Trajectory tracking (at the top) and trajectory tracking error (at the bottom) without noise.

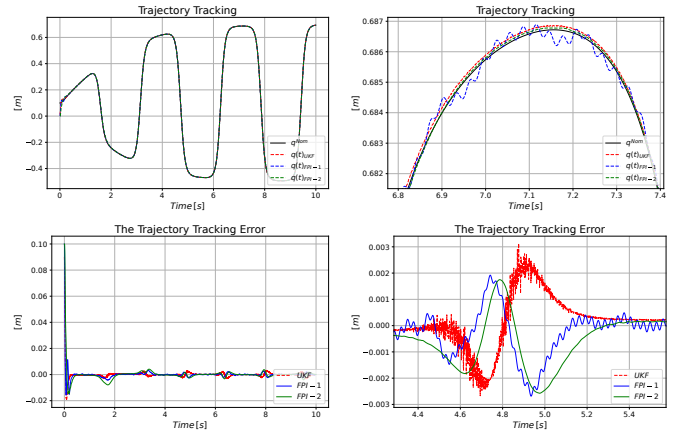


Fig. 5. Trajectory tracking (at the top) and its error (at the bottom) for small amplitude Gaussian noise.

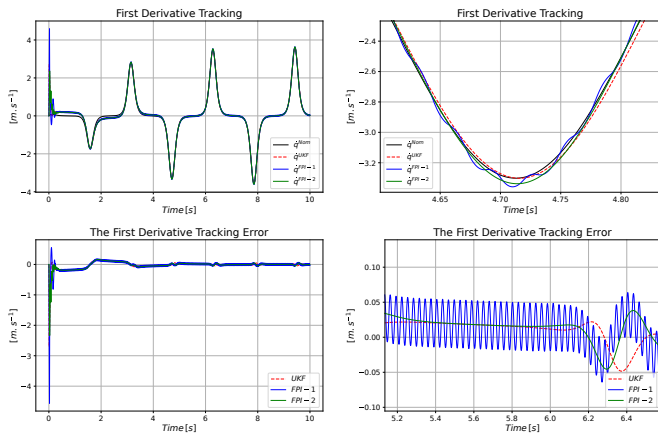


Fig. 3. Tracking the first time-derivative of the trajectory (at the top) and its error (at the bottom) without noise.

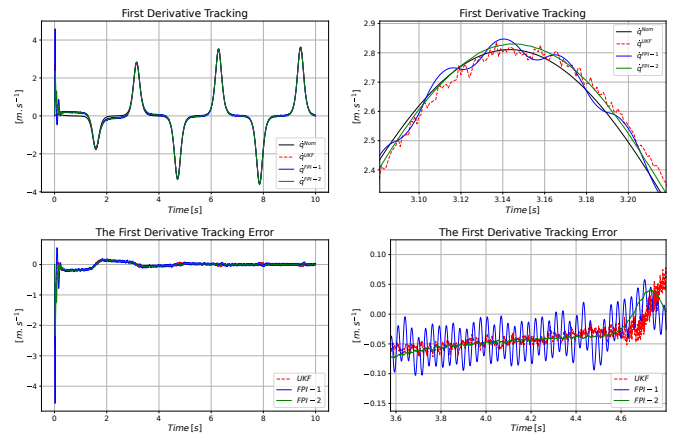


Fig. 6. Tracking of the first time-derivative of the trajectory (at the top) and its error (at the bottom) for small amplitude Gaussian noise.

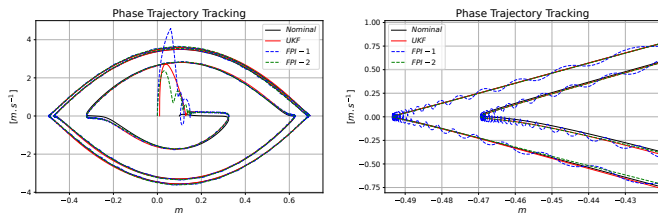


Fig. 4. The phase trajectory tracking without noise.

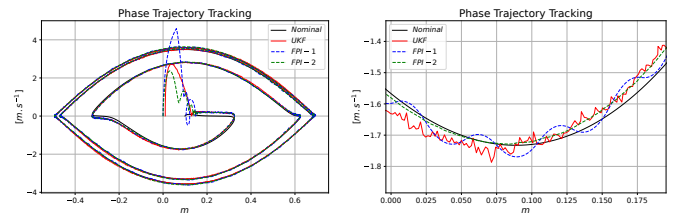


Fig. 7. Phase trajectory tracking for small amplitude Gaussian noise.

### B. Applying Small Amplitude Noise

In this case, the amplitude of applied noise is  $10^{-5}[m]$  in which it will be examined in two cases: Gaussian and Logistic distribution noise. This comparison is important since the Kalman filter is optimized for the Gaussian noise while the other two methods are neutral with regard to the noise distribution.

1) *Small Amplitude Gaussian Distribution Noise:* Figures 5,6,7 reveal that the “smoothest” result was obtained for the simple low pass filter.

The Kalman filter became a little bit hectic, while the continuous fixed point iteration maintained its original fluctuation that was slightly deformed by the noise. However, it yielded the most precise tracking.

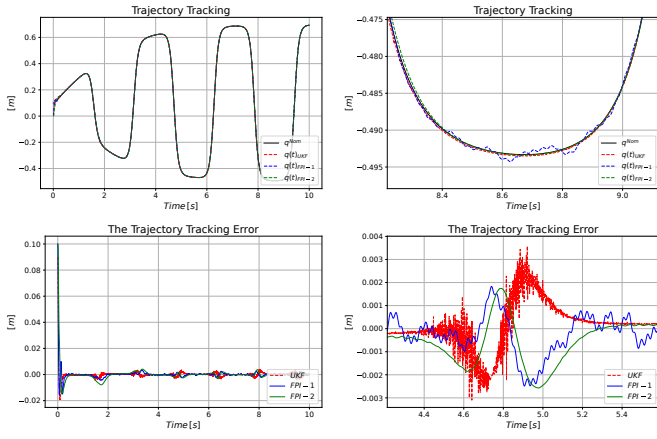


Fig. 8. Trajectory tracking (at the top) and its error (at the bottom) for small amplitude logistic noise distribution.

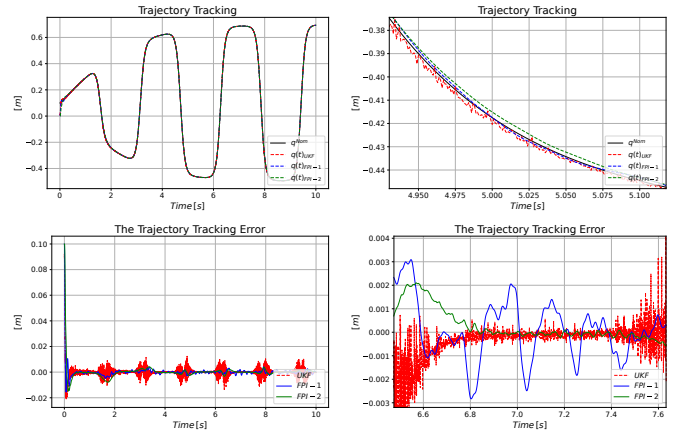


Fig. 11. Trajectory tracking (at the top) and its error (at the bottom) for large amplitude Gaussian noise distribution.

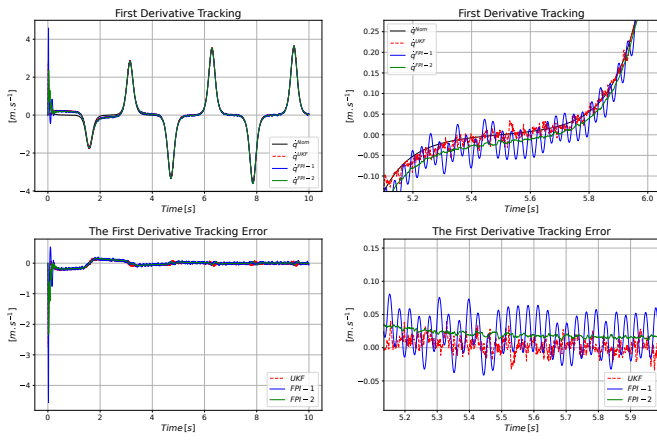


Fig. 9. Tracking the first time-derivative of the trajectory (at the top) and its error (at the bottom) for small amplitude logistic noise distribution.

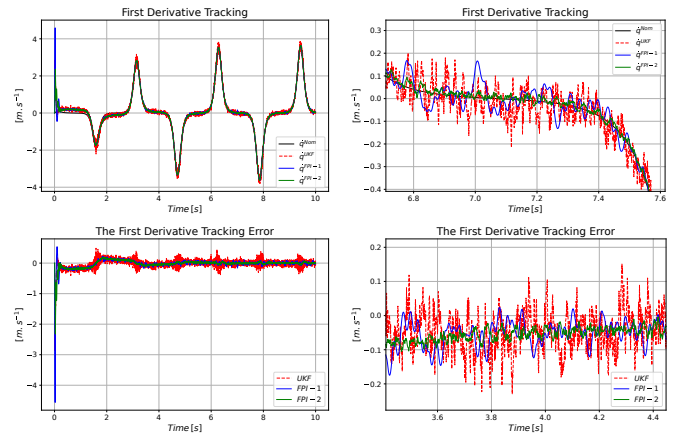


Fig. 12. Tracking the first time-derivative of the trajectory (at the top) and its error (at the bottom) for large amplitude Gaussian noise distribution.

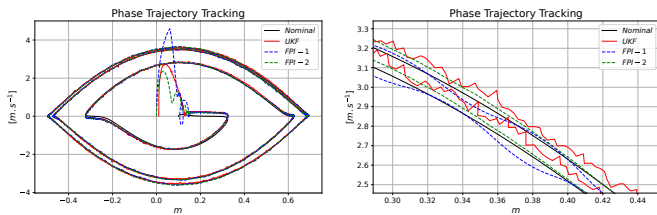


Fig. 10. The phase trajectory tracking for Noise Amplitude =  $10^{-5}$  m.

2) *Small Amplitude Logistic Noise Distribution:* Figures 8,9,10 reveal similar behavior as that of the case of low amplitude Gaussian noise distribution.

C. Applying Large Noise Amplitude

In the simulations of the noise amplitude is  $10^{-4}$  m.

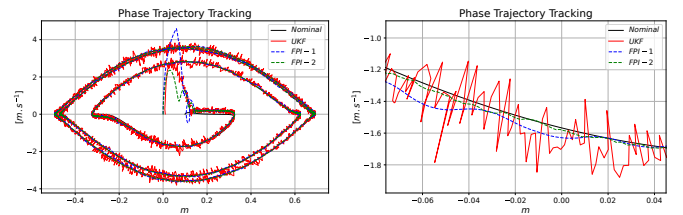


Fig. 13. Phase trajectory tracking for large amplitude Gaussian noise distribution.

1) *Large Amplitude Gaussian Noise Distribution:* Figures 11-13 well testify that the Kalman filter was very sensitive to this noise, it provided hectic result, and the best tracking was achieved again by the use of the simple low pass filter.



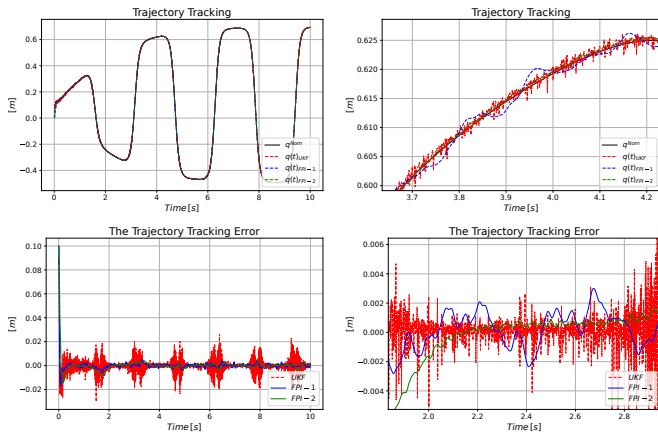


Fig. 14. Trajectory tracking (at the top) and its error (at the bottom) for large amplitude logistic noise distribution.

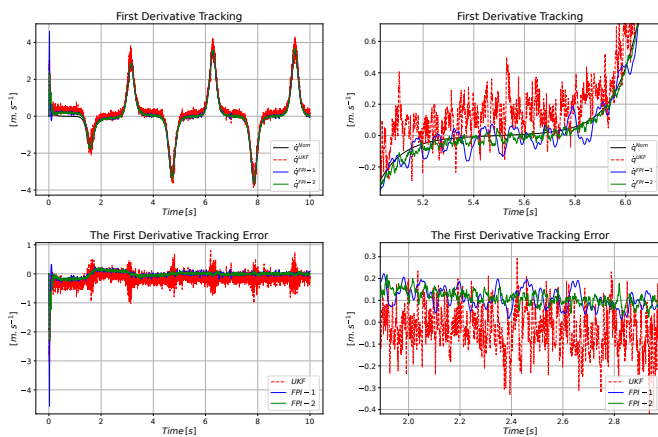


Fig. 15. Tracking of the first time-derivative of the trajectory (at the top) and its error (at the bottom) for large amplitude Logistic noise distribution.

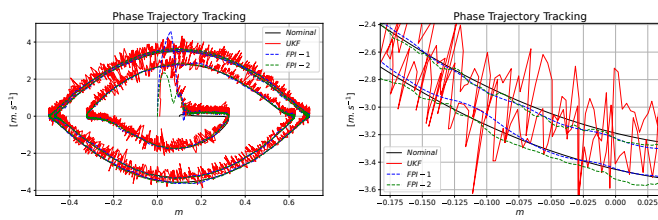


Fig. 16. Phase trajectory tracking for large amplitude logistic noise distribution.

2) *Large Amplitude Logistic Distribution Noise*: Based on Figs. 14,15,16 it definitely can be stated that the Kalman filter provided hectic and imprecise result that manifests itself as some offset in the estimation of the coordinate and its first time-derivative. Again, the best result was obtained for the simple low pass filter.

#### IV. CONCLUSIONS

In this paper via simulation investigations it was revealed that though in general the UKF is a very efficient noise reduc-

tion tool that can be used for the estimation of noisy signals in the control of strongly nonlinear systems, its application to the fixed point iteration-based adaptive control is not expedient. This finding can be explained or understood on the basis of seemingly plausible considerations as follows. The Kalman filter is optimized for Gaussian noise. Behind this fact the tacit assumption is hidden that the noise spectrum is brought about by a large number of unknown and independent factors. However, if the primary cause of the measurement noise is the numerical calculation of the derivatives of the signals of digital encoders, this assumption is not relevant. The usual formulation in the engineering literature that makes a second order system's state propagation equation similar to that of a first order one as  $x_1 = q$ ,  $x_2 = \dot{q}$  do not really work, because these variables are essentially not independent. The Kalman filter is mainly recommended for controlling systems that have really first order dynamical models. Furthermore, it is based on the assumption that the dynamic model is known, and in the case of an adaptive control such an assumption is ab ovo irrelevant.

It was found that much simpler and primitive “heuristic methods” that are not related to the concept of optimization for special noise distribution can provide acceptable results for filtering noisy signals in the *fixed point iteration-based adaptive control*. As the less complicated and less computational power-greedy solution the use of a simple low pass filter with Euler integration can be recommended.

#### REFERENCES

- [1] R. Campa, R. Kelly, and E. García, “On stability of the resolved acceleration control,” *In Proc. of the 2001 IEEE International Conference on Robotics & Automation, Seoul, Korea, May 21-26, 2001*, pp. 3523–3528, 2001.
- [2] M. Mailah, E. Pitowarno, and H. Jamaluddin, “Robust motion control for mobile manipulator using resolved acceleration and proportional-integral active force control,” *International Journal of Advanced Robotic Systems*, vol. 2, no. 2, pp. 125–134, 2005.
- [3] B. Dariush, G. B. Hammam, and D. Orin, “Constrained resolved acceleration control for humanoids,” *In Proc. of the 2010 IEEE/RSJ International Conference on Intelligent Robots and Systems, October 18-22, 2010, Taipei, Taiwan*, pp. 710–717, 2010.
- [4] S. J. Dyke, *Acceleration Feedback Control Strategies for Active and Semi-Active Control Systems: Modeling, Algorithm Development, and Experimental Verification (PhD Dissertation)*. Department of Civil Engineering and Geological Sciences, Notre Dame, Indiana, 1996.
- [5] W. Xu and J. Han, “Joint acceleration feedback control for robots: analysis, sensing and experiments,” *Robotics and Computer Integrated Manufacturing*, vol. 16, pp. 307–320, 2000.
- [6] W. Xu, J. Han, and S. Tso, “Experimental study of contact transition control incorporating joint acceleration feedback,” *IEEE/ASME TRANSACTIONS ON MECHATRONICS*, vol. 5, no. 3, pp. 292–301, 2000.
- [7] Q. Wang, H.-X. Cai, Y.-M. Huang, L. Ge, T. Tang, Y.-R. Su, X. Liu, J.-Y. Li, D. He, S.-P. Du, and Y. Ling, “Acceleration feedback control (AFC) enhanced by disturbance observation and compensation (DOC) for high precision tracking in telescope systems,” *Research in Astronomy and Astrophysics*, vol. 16, no. 8, p. 124, 2016.
- [8] J. Tar, J. Bitó, L. Nádai, and J. Tenreiro Machado, “Robust Fixed Point Transformations in adaptive control using local basin of attraction,” *Acta Polytechnica Hungarica*, vol. 6, no. 1, pp. 21–37, 2009.
- [9] H. Issa and J. K. Tar, “Comparison of various noise filtering techniques in strongly nonlinear adaptive control,” in *IEEE 16th International Symposium on Applied Computational Intelligence and Informatics (SACI 2022) Timisoara, Romania, 2022*, pp. 347–352.

- [10] A. Dineva, J. Tar, and A. Várkonyi-Kóczy, "Novel generation of Fixed Point Transformation for the adaptive control of a nonlinear neuron model," *In proc. of the IEEE International Conference on Systems, Man, and Cybernetics, October 10-13, 2015, Hong Kong (SMC 2015)*, pp. 987–992, 2015.
- [11] A. Dineva, J. Tar, A. Várkonyi-Kóczy, and V. Piuri, "Generalization of a Sigmoid Generated Fixed Point Transformation from SISO to MIMO systems," *In Proc. of the IEEE 19th International Conference on Intelligent Engineering Systems, September 3-5, 2015, Bratislava, Slovakia (INES 2015)*, pp. 135–140, 2015.
- [12] B. Csanádi, P. Galambos, J. Tar, G. Györök, and A. Serester, "A novel, abstract rotation-based fixed point transformation in adaptive control," *In the Proc. of the 2018 IEEE International Conference on Systems, Man, and Cybernetics (SMC2018), October 7-10, 2018, Miyazaki, Japan*, pp. 2577–2582, 2018.
- [13] H. Issa and J. K. Tar, "Noise sensitivity reduction of the fixed point iteration-based adaptive control," in *2021 IEEE 19th International Symposium on Intelligent Systems and Informatics (SISY)*, 2021, pp. 171–176.
- [14] S. Banach, "Sur les opérations dans les ensembles abstraits et leur application aux équations intégrales (About the Operations in the Abstract Sets and Their Application to Integral Equations)," *Fund. Math.*, vol. 3, pp. 133–181, 1922.
- [15] B. Lantos and Z. Bodó, "High level kinematic and low level nonlinear dynamic control of unmanned ground vehicles," *Acta Polytechnica Hungarica*, vol. 16, no. 1, pp. 97–117, 2019.
- [16] E. A. Wan and R. Van Der Merwe, "The unscented Kalman filter for nonlinear estimation," in *Proceedings of the IEEE 2000 Adaptive Systems for Signal Processing, Communications, and Control Symposium (Cat. No. 00EX373)*. IEEE, 2000, pp. 153–158.
- [17] H. M. Menegaz, J. Y. Ishihara, G. A. Borges, and A. N. Vargas, "A systematization of the unscented Kalman filter theory," *IEEE Transactions on Automatic Control*, vol. 60, no. 10, pp. 2583–2598, 2015.
- [18] H. G. De Marina, F. J. Pereda, J. M. Giron-Sierra, and F. Espinosa, "UAV attitude estimation using unscented Kalman filter and TRIAD," *IEEE Transactions on Industrial Electronics*, vol. 59, no. 11, pp. 4465–4474, 2011.
- [19] J. Dunik, M. Simandl, and O. Straka, "Unscented Kalman filter: aspects and adaptive setting of scaling parameter," *IEEE Transactions on Automatic Control*, vol. 57, no. 9, pp. 2411–2416, 2012.
- [20] B. van der Pol, "Forced oscillations in a circuit with non-linear resistance (reception with reactive triode)," *The London, Edinburgh, and Dublin Philosophical Magazine and Journal of Science*, vol. 7, no. 3, pp. 65–80, 1927.
- [21] S. J. Julier and J. K. Uhlmann, "New extension of the Kalman filter to nonlinear systems," in *Signal processing, sensor fusion, and target recognition VI*, vol. 3068. International Society for Optics and Photonics, 1997, pp. 182–193.
- [22] E. Benoît, "Note sur une méthode de résolution des équations normales provenant de l'application de la méthode des moindres carrés à un système d'équations linéaires en nombre inférieur à celui des inconnues (Procédé du Commandant Cholesky)[Note on a Method for Solving Normal Equations Coming from the Application of the Least Squares Method to a System of Linear Equations in Number Less Than That of Unknowns]," *Bulletin Géodésique*, vol. 2, pp. 66–67, 1924.